Density Matrix Generation for 3D Printing

Robert Ulichney[1], Andrew Fitzhugh[2]
HP, Inc, [1]Stow, MA USA, [2]Palo Alto, CA USA

Abstract

A system for creating a rectangular-cuboid periodic matrix for rendering a variable density 3D print is described. This is important for applications where the interior of manufactured objects require less material or weight while still maintaining strength. The matrix elements are grown from a line-based skeleton lattice using a "Line Dilation Algorithm". The method is computationally efficient allowing the design of large matrices to match the resolution and aspect ratio of the 3D printer. A voxel-based halftone model uses the resulting threshold arrays, allowing continuously varying densities. While the method is quite general, the very strong tetrahedral-octahedral lattice is detailed; rendering this triangular structure is made possible by reducing it to a simple rectangular period. Also, rendering constraints preserve structural integrity for multiscale lattices by guaranteeing strut-to-strut connectivity.

Background

In manufacturing physical objects it is often desirable to reduce weight, or reduce the amount of material used. Also, for some additive manufacturing processes reducing the fused material in the core of otherwise solid objects may be important for thermal management. One way to do this is by using a halftone model in 3D. As with 2D halftoning, solutions to the 3D structural halftone problem generally fall into two categories: dispersed and clustered.

Much of the work using the dispersed halftoning approach for 3D focused on the mixture of materials on a local region [1][2]. Direct Binary Search (DBS) halftoning was used to mitigate coarse quantization of surfaces due to layering [3]. However while it can reduce density, the irregular nature of dispersed halftoning does not preserve strength.

The parallel to 2D clustered-dot halftoning would be a connected lattice in 3D. There is a rich background of work that use a vector-based, rather than a voxel-based, approach to build periodic microstructures. "Intralattice" is software that fabricates lattice-skin structures based on a method for generating lattice meshes [4]. With the goal of minimizing weight, methods include designs based on isotropic unit cells [5], hollow-tube lattices [6], and an analytical model of unit lattices to compose larger structures [7]. To expand the range of material properties the geometry of the periodic lattice design can be made to evolve to minimize stress concentrations [8], or enhance the compressibility of graphene microlattices [9]. There is even work with aperiodic structures to achieve orthotropic elastic behavior [10] where a fine-scale foam-like structure is developed using a stochastic process with independent elasticity properties along the three orthogonal axis.

Lattice-based structures defined by vector-based shapes are one approach but do not lend themselves easily to continuously varying densities. To address the need for variable density and strength we propose a means for producing a 3D density threshold matrix by dilating a line-based skeleton specification, along with proposing a particularly strong skeleton structure. A voxel-base halftone system can then efficiently render continuously varying densities to accommodate the target structural requirements.

The Tetrahedral-Octahedral Lattice

One of the strongest structural lattices is the one formed by the segments connecting the centers of optimally packed equi-sized spheres. Spheres can be so packed in two ways as shown in Figure 1.

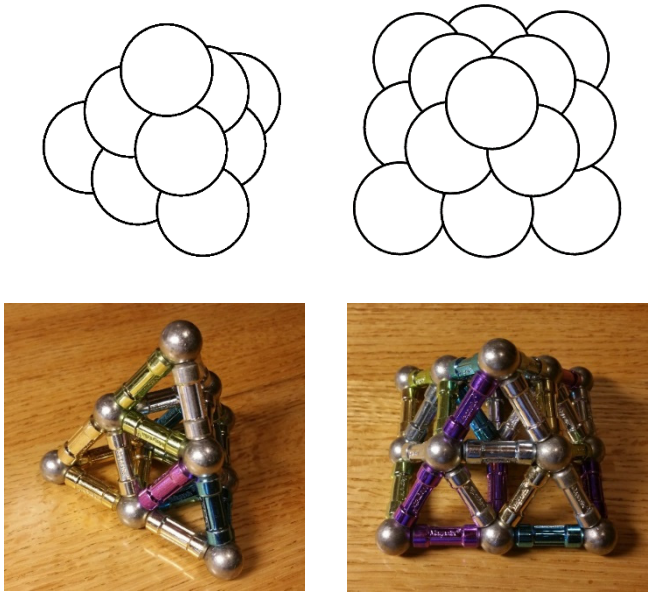

Figure 1. Triangular (left) and square (right) Pyramid Sphere Packing structures.

One is triangular pyramid sphere packing and is depicted in (a) as the pattern formed by packing spheres with a base that forms a triangle; next to that is a model of the underlying lattice suggested by that arrangement. (The triangular packing method can also be described as hexagonal packing.) The other possibility is square pyramid sphere packing as shown in Figure 1(b). Note that in both cases the line segments are all the same length.

While these packing strategies may be described as different, it is important to point out that they are exactly the same in tessellating space. They differ only by an angle of rotation θ around an axis defined by any horizontal segment in either the triangular or square pyramids. Figure 2(a) shows a portion of the triangle pyramid with horizontal base ABC. The blue lines represent equal segments of length one. The dotted black lines are perpendicular segments. The angle ∠DAE= θ is the angular difference between a triangular pyramid and a square pyramid. In Figure 2(b) the equilateral triangle ABC is shown with perpendicular bisectors.

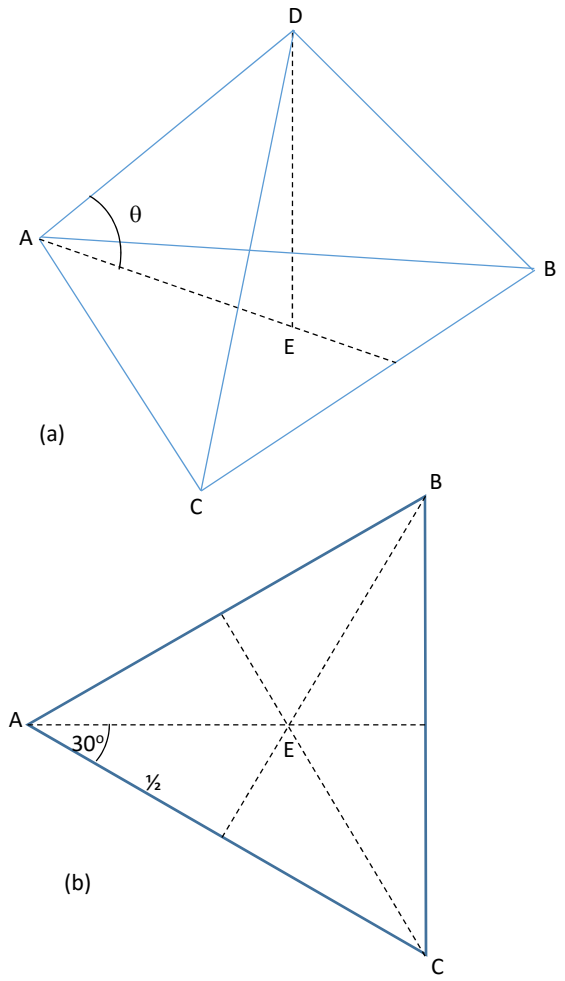

Figure 2. Portion of a triangular pyramid lattice.

The length of segment

$$\overline{AE} = ½ / \cos(30^o) = \sqrt{3}/3.$$

The angle then is

$$\theta = \cos^{-1}(\overline{AE} / \overline{AD}) = \cos^{-1}(\sqrt{3}/3) \approx 54.7^o.$$

In either case, triangular or square, the he structure is called a tetrahedral-octahedral lattice based on the shapes of the volumes outlined by the line segments. A key step to building a single repeating matrix is to find a rectangular-cuboid period that will tessellate all of three-space with this lattice. The solution is the line set shown in Figure 3. The red lines indicate those lines that are part of neighboring periods. The period has a dimensional ratio x:y:z of 1:1:√2.

Density Matrix Generation by Line Dilation

Starting with a line-based skeleton such as the one described above, we build a rank matrix based on the distance each element is from this skeleton. We call the method the "Line Dilation Algorithm".

The size of the period is expressed relative the x dimension, as $1:s_y:s_z$. For the tetrahedral-octahedral lattice example $s_y = 1$, $s_z = \sqrt{2} \approx 1.414$. The line-based skeleton is expressed as a list of lines defined by two end points inside a unit volume.

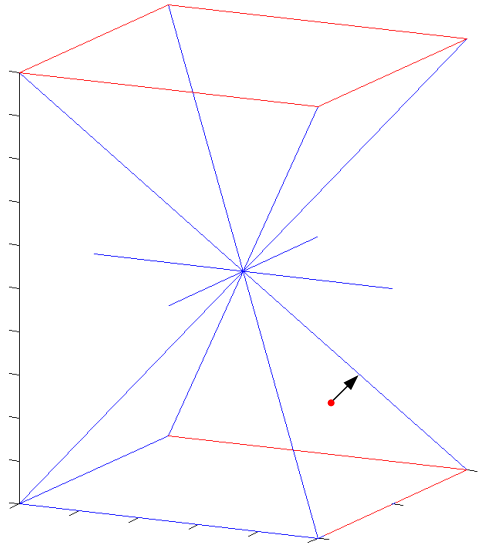

Figure 3. Line Skeleton of a Rectangular-cuboid Period.

The size of the Density Matrix is specified by one variable, the size in X. The other two dimensions are determined by the printer's voxel aspect ratio, and period size s_y and s_z. The voxel aspect ratio is a property of the target printer. For example, if a printer has an x and y voxel pitch of 1234 samples per inch, and a z resolution of 260 samples per inch, the voxels would be longer in the z direction by 1234/260 than they are in x or y. The voxel aspect ratio is expressed relative to the size in x as v_y and v_z. Continuing the example, $v_y = 1$ and $v_z = 1234/260 \approx 4.746$. Combining this data, the matrix dimensions are

$$X,\ Y = Xs_y/v_y, \text{ and } Z = Xs_z/v_z.$$

Using these values, for a specified size of X = 300, the other dimensions after rounding would be Y = 300 and Z = 89.

For each point in the matrix, such as that shown by a red dot in Figure 3, we first find the distance to each line in the skeleton. This is achieved with the help of Figure 4(a) where $\mathbf{p}_1$ and $\mathbf{p}_2$ are two points on one of the skeleton lines and $\mathbf{p}$ is the matrix element. For each element, or point $\mathbf{p}$, we need to find the distance to each line in the line-based skeleton. The general problem of finding the closest distance from a point to a line defined by two other points is illustrated in Figure 4(b). We need to find the distance d from point $\mathbf{p}$ to the line defined by the two points $\mathbf{p}_1$ and $\mathbf{p}_2$ in three dimensional space.

We define two vectors $\mathbf{a}$ and $\mathbf{b}$:

$$\mathbf{a} = \mathbf{p}_1 - \mathbf{p}_2$$
$$\mathbf{b} = \mathbf{p} - \mathbf{p}_2$$

where the magnitudes are

$$a = |\mathbf{a}|, \text{ and } b = |\mathbf{b}|.$$

The key is utilizing the geometric relationship involving the magnitude of the vector cross product:

$|\mathbf{a} \times \mathbf{b}|$ = area defined by the parallelogram (yellow in the figure)
= da

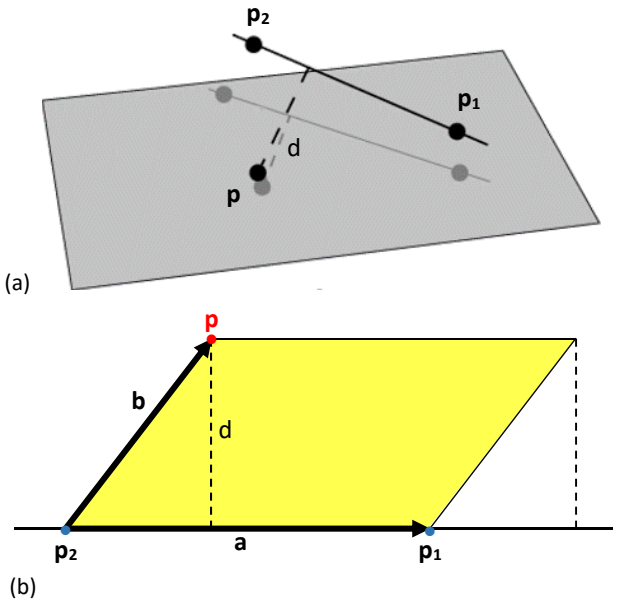

Figure 4. Finding the closest distance from a point to a line.

Thus,

$$d = |\mathbf{a} \times \mathbf{b}| / a$$

Since **a**, a, and $\mathbf{p}_2$ are constants for the independent variable **p**, the operational equation is

$$d = |\mathbf{a} \times (\mathbf{p} - \mathbf{p}_2)| / a$$

The distance to the closest line is recorded at each location, then those distances are sorted from smallest to largest producing a rank matrix. The resulting density threshold matrix is then the rank matrix normalized by the range of values used to specify the input density. Similar to growing dots in 2D clustered-dot halftone generation where dots are dilated as the input gray value increases, the density matrix dilates the skeleton lines as density increases.

The use of a periodic rectangular-cuboid threshold array allows for a very efficient run-time rendering system. The voxel vs. no-voxel state for each addressable printed position is determined by a simple threshold operation against the input density value. In Figure 5 the rendering system generated four bistate output objects for fixed density inputs with values as indicated. The size of the objects are exactly 2x2x2 periods to show the nature and periodicity of the dilated structures. For the case of an input density of 99% the output is best visualized by the remaining empty space or holes colored red in the figure. As an example of a variable density input object, consider a sphere with a 10% density in the center gradually increasing to 100%, or solid, density at the outer surface. A radial cross section of part of that input object is depicted with gray scale representing density in Figure 6. One octant of the rendered bistate output is shown in Figure 7.

In Figure 8 this matrix was used with a 3D printer to produce 25% density prints with ½-inch and ¼-inch struts. Figure 9 is another example cross-section print where in this case the input density varies from 15% in the center to 100%, or solid, at the outer shell. In all cases, the bistate output of the density threshold operation can be thought of as a placeholder to be filled by any material or mixture of material; in figure 9 color is one of the variables.

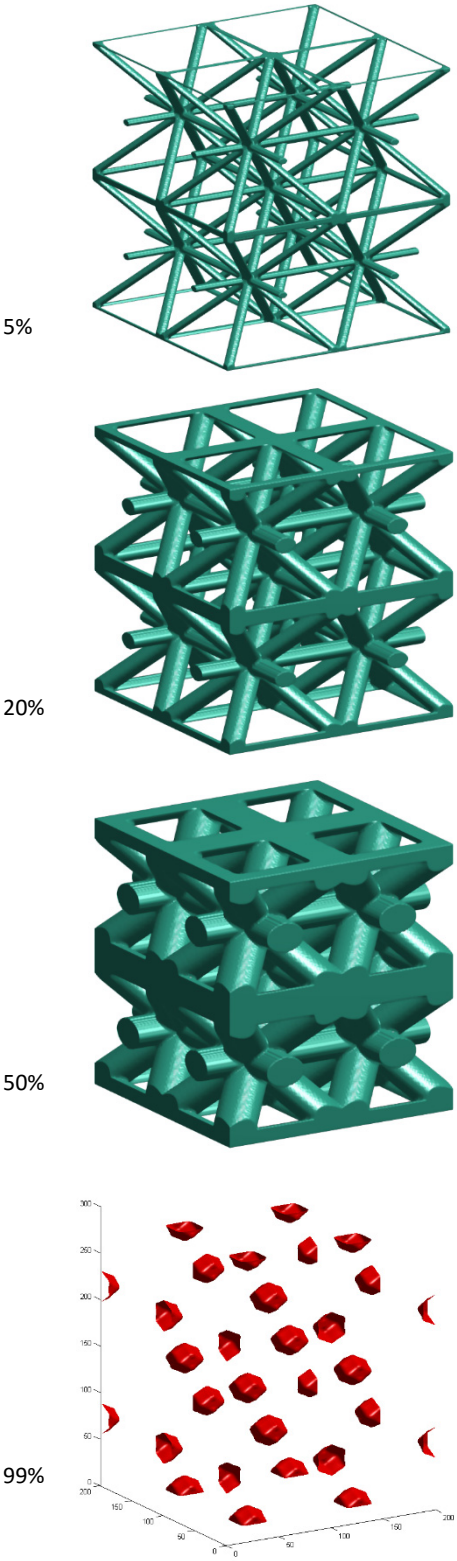

Figure 5. 2x2x2 period output for different densities.

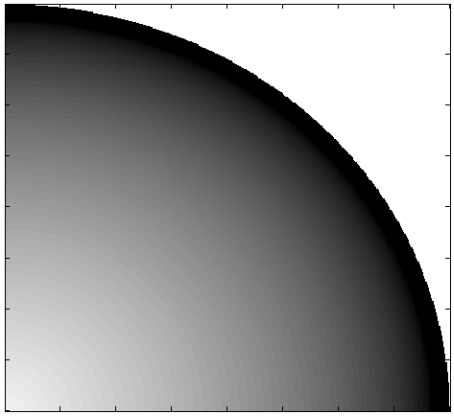

Figure 6 Radial cross section of density map of a sphere.

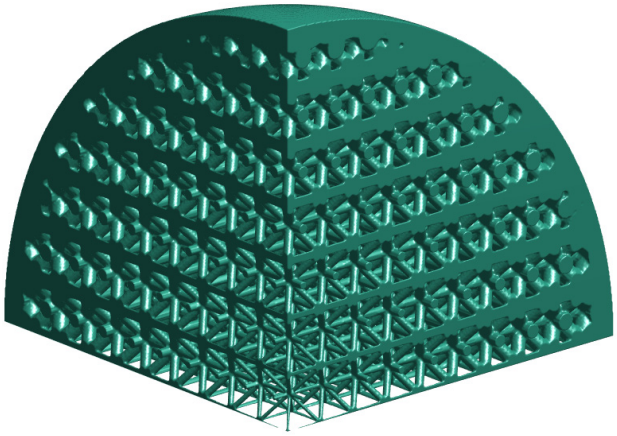

Figure 7. One octant of the output object of a variable density sphere input.

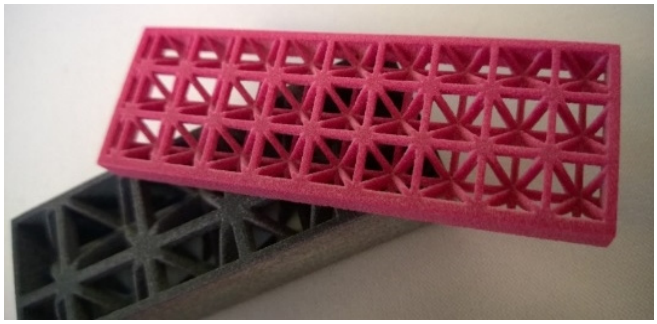

Figure 8. 25% density with ½" and ¼" struts.

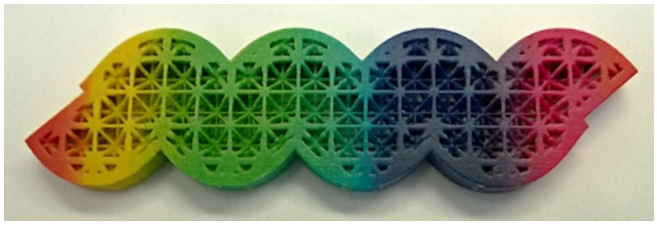

Figure 9. Print varying in density from 15% to 100%.

Multiscale Solution

Variable Density lattices are useful for filling the interiors of 3D printed objects for both reducing weight and thermal management during fabrication. However one lattice size is not always appropriate for all interior volumes. Smaller or more confined interior volumes are served better by smaller lattice structures and larger more open interior volumes by larger lattice structures. For objects that have both tight and spacious interior spaces it would be useful to change lattice sizes in the same object. The problem is that the interface between lattice changes can be very weak. An example of is shown in Figure 10(a) where a larger tetrahedral lattice transitions to a smaller cubic lattice. Because the aspect ratios of the rectangular periods of the two structures are not the same it will generally be the case that struts from one lattice will not attach to struts from the other lattice. In Figure 10(b) both the larger and smaller lattice are of the same type, and there is even an integer relationship between the scale of each lattice. However the general case will be that the struts from one lattice will not connect to other, as shown. In both of these examples the shell of the 3D print enveloping these interiors will carry the entire stress holding the object together. Without a shell, these structures would fall apart and separate at the interface between lattices, negating any strength benefit afforded by using a lattice fill in the first place. We seek a solution where a variable density fill structure can be multiscale and still maintain strength at the interfaces.

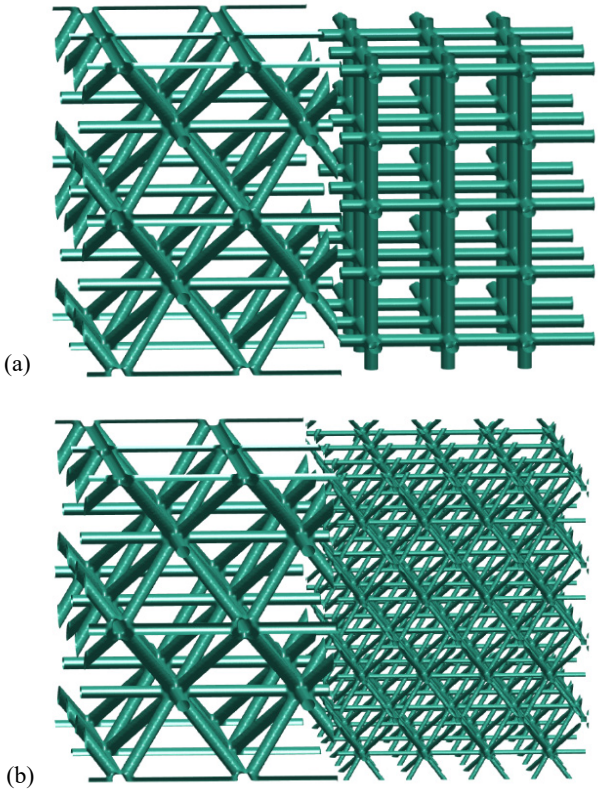

Figure 10. Typical interface failure.

This is achieved by forcing finer scaled versions of the lattices to line up with coarser versions. Consider a two-dimensional slice of the solution as shown in Figure 11 where the extent of lattice periods are outlined. (An actual shape of a lattice is not shown.)

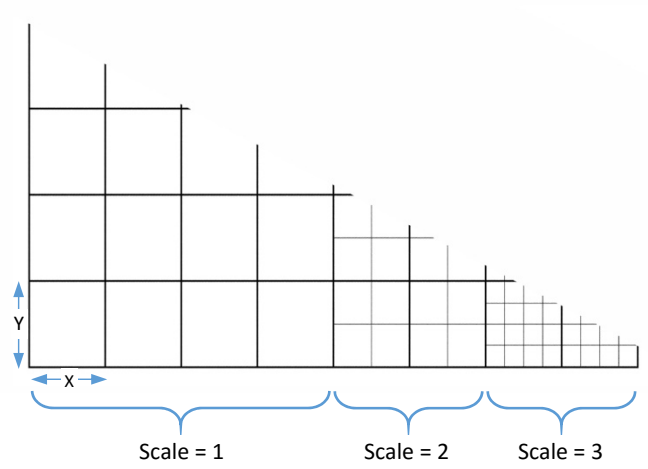

Figure 11. Assigning Lattice scales as a function of Spaciousness.

The density lattice is represented by an X by Y repeating period depicted by the dark lines in the figure. The group of periods labeled Scale = 1 represent the largest scale where a single instance of the lattice fills each X by Y period. The group of periods labeled Scale =2 each have exactly 2x2 smaller versions of the original structure. Likewise the group labeled Scale =3 each have 4x4 smaller versions of the original structure. In this example larger lattices fill the more spacious area and smaller lattices fill the less spacious area. Structural integrity is achieved by forcing scale changes to only occur at the border of the fundamental X by Y period, and by making smaller versions of the lattice with the same shape as larger versions.

A visualization of the first three scales of the threshold matrices designed in this way is shown in Figure 12, depicting structures that could be rendered by those matrices. All the matrices are the same size. A key benefit of this strategy of allowing matrix change at fundamental period boundary is that struts from the larger scale will always connect with struts of a smaller scale. Figure 13 illustrates the well connectedness between two scales using this strategy for the example of (a) a tetrahedral lattice, and (b) a cubic lattice. Photos of printed examples of this approach for both a tetrahedral and cubic density threshold matrices are illustrated in Figure 14 using three different scale lattices.

Variable density 3D objects printed using threshold matrices generated with the Line Dilation algorithm can replace solid fill volumes without compromise to structural integrity. By identifying a rectangular-cuboid period that tessellates a volume with the tetrahedral-octahedral lattice, a simple matrix halftoning model can fill a volume with a strong fill using less mass. Both density and scale can change to accommodate a wide range of 3D prints.

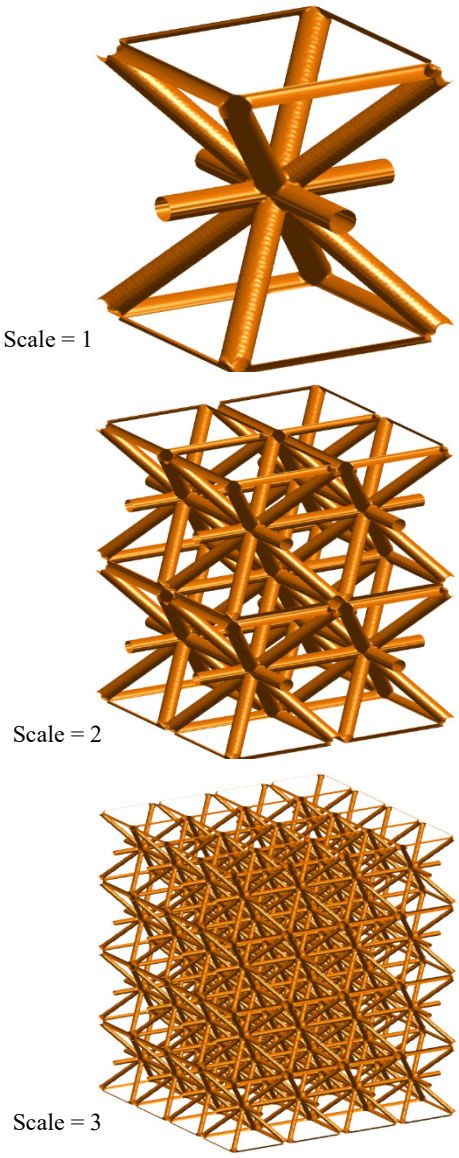

Figure 12. Visualization of multiscale Threshold Matrices

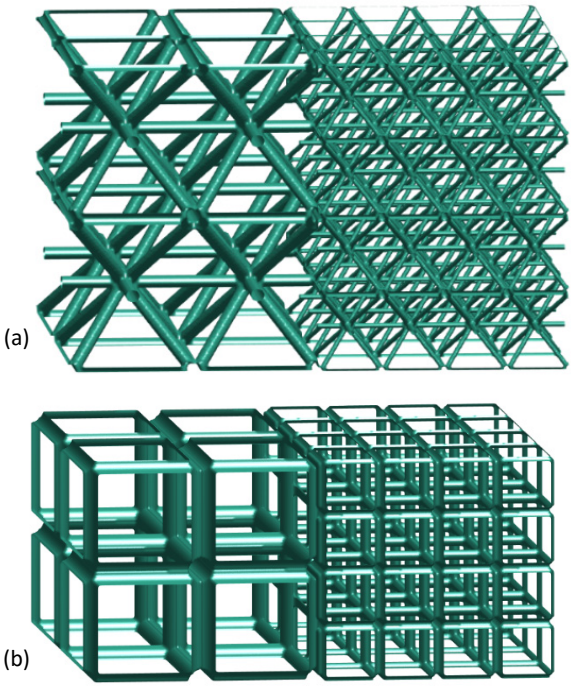

Figure 13. The interface between matrices of two different scales. (a) Tetrahedral Matrices, (b) Cubic Matrices.

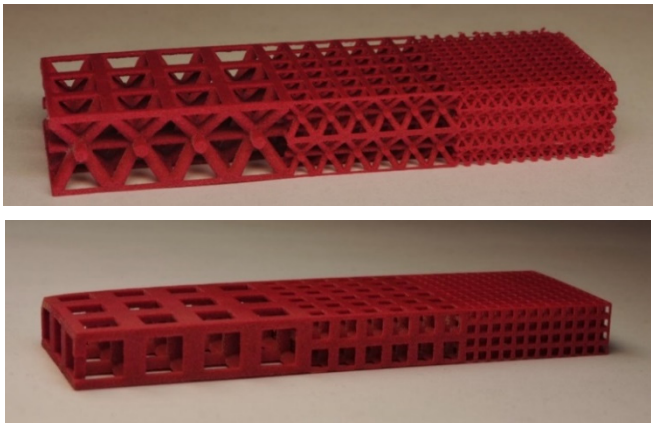

Figure 14. Multiscale Density prints using tetrahedral (top) and cubic (bottom) matrices.

References

[1] W. Cho, et al. "Methods for distributed design and fabrication of parts with local composition control." *Proceedings of the 2001 NSF Design and Manufacturing Grantees Conference*, 2001.

[2] W. Cho, E. Sachs. N. Patrikalakis, D. Troxel, "A Dithering Algorithm for Local Composition Control with Three-Dimensional Printing", MIT Design Laboratory Memorandum 2001-3, revised 2002.

[3] C. Zhou, Y. Chen, "Three-Dimensional Digital Halftoning for Layered Manufacturing Based on Droplets", *Trans. of NAMRI/SME*, 2009.

[4] Y, Tang, Y. Zhao, "Lattice-skin Structures Design with Orientation Optimization", Proceedings of the International Solid Freeform Fabrication (SFF) Symposium, pp. 1378-1393, Austin, TX, Aug 10-12, 2015.

[5] X. Zheng, et al., "Ultralight, ultrastiff mechanical metamaterials", *Science*, Vol. 344, Issue 6190, pp. 1373-1377, Jun, 2014.

[6] T. Schaedler, et al., Ultralight metallic microlattices, *Science*, Vol. 334, pp. 962–965, 2011.

[7] D. Rosen, S, Johnston, M. Reed, "Design of general lattice structures for lightweight and compliance applications", In *Proc. Rapid Manufacturing Conference*, pp. 1–14, July 5-6, 2016.

[8] J. Panetta, A. Rahimian, D. Zorin, "Worst-Case Stress Relief for Microstructures", *ACM Transactions on Graphics*, Volume 36 Issue 4, July 2017.

[9] C. Zhu, et al., "Highly compressible 3D periodic graphene aerogel microlattices", *Nature Communications*, Vol. 6, Article number: 6962, Apr. 2015.

[10] J. Martinez, H. Song, I. Dumas, "Orthotropic k-nearest foams for additive manufacturing", *ACM Transactions on Graphics*, Volume 36 Issue 4, July 2017.

Author Biography

Robert Ulichney is a Distinguished Technologist with HP Labs focusing on systems for high capacity data embedding, and structures for variable density 3D printing. He received a Ph.D. from MIT in electrical engineering and computer science, and is a Fellow with IS&T. Before joining HP he was with Digital Equipment Corp then with Compaq's Cambridge Research Lab. His publications are available at ulichney.com.